FRACTURE MECHANICS OF THE MICROBOND AND PULL-OUT TESTS

JOHN A. NAIRN

INTRODUCTION

The properties of the fiber/matrix interface in composites have an influence on their overall performance. Common methods for studying the interface are micromechanical tests that load a single fiber/matrix interface to failure. Two popular tests are the microbond test [1] and the single-fiber, pull-out test [2]. In a microbond test a droplet of matrix is sheared off the fiber by pulling the fiber while restraining the droplet. In a pull-out test, the end of a fiber is embedded in a polymer and pulled until failure while restraining the matrix. A common interpretation of these tests is to reduce the load at failure to an interfacial shear strength (ISS) by dividing the applied load by the total interfacial area. Physically this term is the average interfacial shear stress at the time of failure. ISS has some use in qualitative work; it is less useful for fundamental characterization of the interface.

An alternative approach is use fracture mechanics methods. In each test, a crack initiates and propagates along the fiber matrix interface. By analyzing the interfacial cracking process with fracture mechanics, it is possible to determine an interfacial toughness instead of an ISS. The key analysis problem is to solve for the energy release rate of a propagating crack. The resulting equations can then be used to interpret experimental results. Two complicating features are residual stresses and friction. Residual stresses are always important in composites due to differential shrinkage between the fiber and the matrix. Friction is important in microbond and pull out tests because of the predominantly mode II loading conditions. This chapter presents a fracture mechanics model for both tests that includes all relevant effects. The model has been used to interpret experimental results.

FRACTURE MECHANICS THEORY

Detailed stress analysis of interface cracks is a difficult problem that has received much attention [3]. Fortunately, good results can be obtained for microbond and pull-out specimens by using an approximate, global energy analysis rather than a local, interfacial crack tip analysis. This section summarizes an analysis for energy release rate due to crack growth in microbond and pull-out specimens. More details can be found in Refs. [4-6].

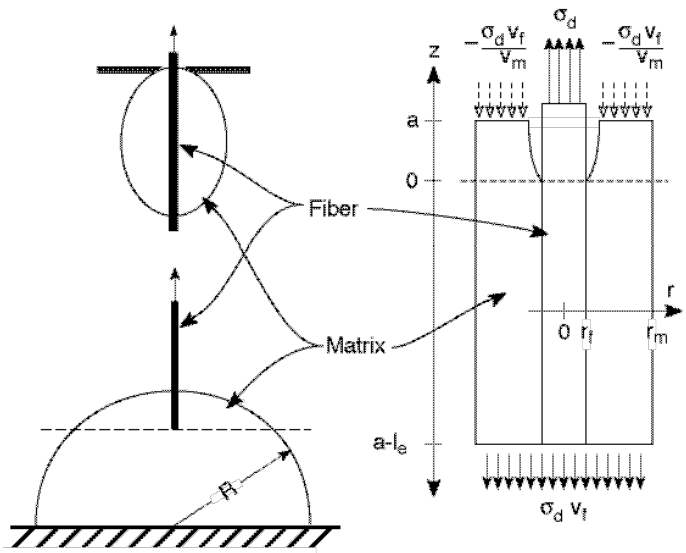

Fig. 1. The left side shows the microbond (top) and pull-out (bottom) specimen geometries. The right side shows the equivalent concentric cylinder model where the embedded length of fiber is in a cylinder of matrix. The fiber in both specimens is loaded with stress σ_d. The "dotted"' arrows are the remaining microbond specimen boundary conditions; the solid arrows on the bottom of the specimen are the remaining pull-out specimen boundary conditions.

Figure 1 shows a reduction of real specimens to an idealized geometry more amenable to analysis [4,5]. The simplification for the pull-out test is to replace the matrix region surrounding the embedded fiber by an equivalent cylinder of matrix. The length of the cylinder is equal to the embedded fiber length, l_e. The radius, r_m, is chosen to preserve the total fiber volume fracture, v_f, within the zone of the embedded fiber. The energy release rate analysis can thus focus on the concentric cylinder model on the right of Fig. 1 because neither the free fiber outside the matrix nor the matrix zone below the fiber end release energy during crack growth. The pull-out specimen is loaded by a fiber stress of σ_d. By force balance, the total stress on the bottom of the specimen is $\sigma_d v_f$. The simplification for the microbond specimen is to replace the elliptical matrix droplet by a matrix cylinder with length equal to the embedded fiber length and matrix radius chosen to preserve the total fiber volume fraction within the matrix. The microbond specimen is loaded by fiber stress of σ_d at the top of the specimen; that stress is balanced by a matrix stress of $-\sigma_d v_f/v_m$. The bottom of a microbond specimen is stress free.

Applying the general composite fracture mechanics methods from Ref. [6] to the idealized geometry in Fig. 1 with an interfacial debond of length a, the energy release rate for debond growth in both specimen types can be written as

$$G(a) = \frac{r_f}{2}\left[C_{33s}\bar{\sigma}^2 + 2D_{3s}\bar{\sigma}\Delta T + \left(\frac{D_3^2}{C_{33}} + \frac{v_m(\alpha_T - \alpha_m)^2}{v_f A_0}\right)\Delta T^2\right.$$
$$\left.\left(\frac{mv_f\sigma_d}{2}\left(\frac{1}{E_A} - \frac{1}{E_m}\right) + D_{3s}\Delta T\left(\frac{2\alpha_f}{r_f}C_T(a) - \bar{\alpha}\right) + \frac{(1+m)D_3\Delta T}{C_{33}}C_T'(a)\right)\right] \quad (1)$$

where m=0 or 1 is for pull-out or microbond tests, respectively. The term $\bar{\sigma}$ is a reduced debonding stress defined by

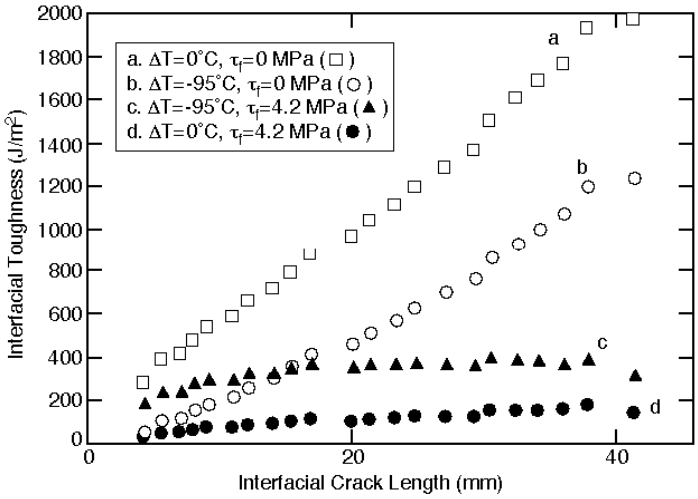

Fig. 2. Crack-resistance curves for a steel/epoxy model specimen analyzed four different ways. Curve *a* ignores residual stresses and friction; curve *b* includes residual stresses but ignores friction; curve *c* includes both residual stresses and friction; curve *d* ignores residual stresses, but includes friction.

$$C_T(a) = \int_0^{l_e - a} F(z)\,dz \tag{3}$$

where $F(z)$ is the solution for axial fiber stress in concentric cylinders of length l_e-a subjected to unit normal stress on the fiber and a balancing $-v_f/v_m$ stress on the matrix, both at $z=0$ in addition to zero stress on the other end at $z=l_e$-a. The functions $F(z)$ and $C_T(a)$ can be found by any analytical, numerical, or even experimental means and then substituted into Eq. (1) to find the energy release rate. One simple analytical approach, which was demonstrated to be accurate by comparison to finite element analysis [4,6], is to use shear-lag analysis for which it is easy to derive [4]:

$$C_T(a) = \frac{1}{\beta}\left[\coth\beta(l_e - a) - \operatorname{csch}\beta(l_e - a)\right] \tag{5}$$

where β is a shear-lag parameter as defined in Ref. [4] and elsewhere.

MICROBOND AND PULL OUT EXPERIMENTAL RESULTS

Verification of fracture mechanics methods for the microbond test was done using macroscopic model specimens of a steel wire embedded in a cylinder of epoxy (see Ref. [4] for specimen details). Steel/epoxy specimens are analogues of carbon/epoxy or glass/epoxy microscopic specimens with modulus ratio similar to carbon/epoxy but higher than glass/epoxy specimens. In macroscopic experiments, crack growth along the interface could be observed visually. After debonding was complete, it was further possible to observe and record frictional stress. The key experiments are force as a function of crack length for various specimen geometries. The verification experiments are summarized in Fig. 2 in which the raw data are interpreted by fracture mechanics four different ways. For fracture mechanics to be useful, one expects the measured toughness to be independent of geometrical factors and of crack length. Microbond experiments satisfy this requirement provided the data are analyzed correctly.

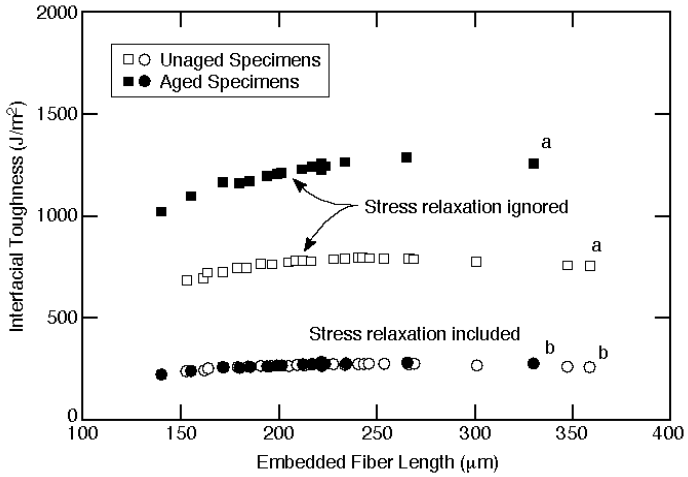

Fig. 3. Fracture toughness calculated from microbond specimens as a function of droplet length. Curves *a* include residual stresses but do not account for relaxation of those stresses during aging. Curves *b* account for relaxation of residual stresses.

Curve *a* in Fig. 2 is an analysis that ignores both residual stresses and interfacial friction. This curve is clearly a poor fracture mechanics result. Curve *b* includes residual thermal stresses by setting ΔT=-95˚C, but still ignores friction; it is also a poor fracture mechanics result. Curves *c* and *d* both include friction effects by setting τ_f=4.2 MPa which was the measured interfacial shear stress after complete debonding. Curve *c* is an analysis that included both residual stresses and friction. This curve is a good fracture mechanics result. There is an initial rise in toughness at short debond lengths, but the results soon level out at an approximately constant toughness (360 J/m^2). Curve *d* includes interfacial friction, but ignores residual stresses. Although curve *d* looks relatively flat on the scale of Fig. 2, it actually never levels off and is a poor fracture mechanics result. The difference between curves *c* and *d* illustrates the magnitude of the contribution of residual stress to debonding. The magnitude is large; in fact, most of the energy released comes from residual stresses.

The experiments are more difficult with micro-specimens because it is difficult or impossible to observe crack growth. From the macroscopic specimen results, and in agreement with theory, it was found that interfacial crack growth is stable and the load continued to increase until complete debonding. A proposed fracture mechanics approach when there is no crack length data is to record the peak load and calculate interfacial toughness from Eq. (1) by taking the limit as *a* approaches droplet length [4-6]. This approach was verified by using it on the macroscopic experiments for which crack length could be observed. The toughness calculated by the peak-load method agreed reasonably well with a full analysis that included crack-length information. Figure 3 shows an experimental investigation of the effect of aging on interfacial toughness from micro-sized E-glass fiber/epoxy specimens [6,8]. These data were analyzed by the peak-load method. Fracture mechanics analysis should show a toughness that is independent of droplet length and differences between aged and unaged results should show the effect of physical aging on the interfacial toughness. The square symbols are an initial fracture mechanics analysis that used a simplistic calculation of residual stresses. These results gave the impression that the interfacial toughness increased with aging. Similarly, a non-fracture mechanics method suggested that aging affected the interface. The true results were revealed by new fracture mechanics calculations that included the actual level of residual stresses by accounting for stress relaxation during the aging process. The final interpretation (circular

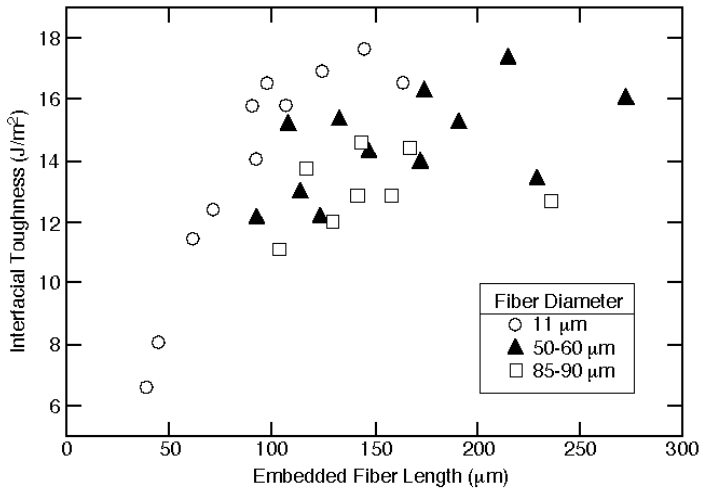

Fig. 4. Fracture toughness calculated from initiation of debonding in pull-out tests for glass fibers of three different diameters in a vinyl-ester matrix as a function of embedded fiber length.

symbols) showed that aging does not affect interfacial toughness; it only changes the level of residual stresses. These experiments illustrate how fracture mechanics interpretation can lead to the proper interpretation of experiments, but it is essential to have a good energy release rate analysis and to include all significant effects such as residual stresses and friction.

Fracture mechanics can analyze pull-out tests by similar methods. In the pull-out results for glass fiber/vinyl ester [9] analyzed in Fig. 4, it was possible to observe initiation of crack growth as a kink in the load-displacement curve. A toughness was calculated from each specimen using Eq. (1) by setting a=0 (or any suitably small a). Friction could be ignored because it had a negligible effect for initiation. The effect of friction only becomes significant as the debond length gets long. The calculated interfacial toughness for three fibers of different diameters is plotted in Fig. 4 as a function of embedded fiber length. After an initial rise, all results became roughly constant. In other words, as expected for good fracture mechanics results, the interfacial toughness was independent of both fiber length and fiber diameter.

RECOMMENDATIONS

Equation (1) provides an accurate, analytical result that can be used to calculate the energy release rate for interfacial crack growth in both the microbond and the pull-out test geometries. Hence, it is possible to derive fracture toughness information from these common interfacial test methods. The calculation of interfacial toughness requires sufficient experimental input for determination of all terms in Eq. (1). The key results needed are specimen geometry, current interfacial crack length, the load required to extend the crack, the actual level of residual stresses, and the magnitude of any friction on the debond surfaces. Residual stresses are particularly important for analysis of microbond specimens because they account for much of the energy released. Friction is especially important as the debond gets long. In some micro-sized specimens it can be difficult to observe crack growth. This situation can be handled by using indirect means to deduce crack length. For example, the crack length at the peak load in microbond tests is nearly equal to the droplet length. For pull-out tests, debond initiation can sometimes be observed as a kink in the force-displacement curve and the “kink” load corresponds to zero initial crack length.

REFERENCES

1. B. Miller, P. Muri, and L. Rebenfeld (1987) *Comp. Sci. & Tech*. **28**, 17-32.
2. L. S. Penn and E. R. Bowler (1981) *Surf. Interf. Anal.* **3**, 161-164.
3. M. L. Williams (1959) *Bull. of the Seismological Society of America* **49**, 199-204.
4. C. H. Liu and J. A. Nairn (1999) *J. of Adhes. & Adhesives* **19**, 59-70.
5. J. A. Nairn (2000) *Adv. Comp. Letts.* **9**, 373-383.
6. J. A. Nairn (2001) *Proc. 16th Ann. Tech. Conf. Amer. Soc. Composites*, Sept. 9-12, 2001, Blacksburg, VA.
7. J. A. Nairn (2000) *Int. J. Fract.* **105**, 243-271.
8. D.-A. Mendels, Y. Leterrier, J.-A. E. Månson, and J. A. Nairn (2003) *J. Comp. Mat*. in press.
9. S. Zhandarov, E. Pisanova, E. Mader, and J. A. Nairn (2000) *J. Adhesion Sci. & Tech.* **15**, 205-222.